Integrated omics approach for the identification of HDL structure-function relationships in PCSK9-related familial hypercholesterolemia

Maryam Darabi, Marie Lhomme, Maharajah Ponnaiah, Maja Pučić-Baković, Isabelle Guillas, Eric Frisdal, Randa Bittar, Mikaël Croyal, Lucrèce Matheron-Duriez, Lucie Poupel, et al.

Integrated omics approach for the identification of HDL structure-function relationships in PCSK9-related familial hypercholesterolemia

Maryam Darabi, PhD, Marie Lhomme, PhD, Maharajah Ponnaiah, PhD, Maja Pučić-Baković, PhD, Isabelle Guillas, PhD, Eric Frisdal, PhD, Randa Bittar, PhD, Mikaël Croyal, PhD, Lucrèce Matheron-Duriez, PhD, Lucie Poupel, PhD, Dominique Bonnefont-Rousselot, PhD, Corinne Frere, PhD, Mathilde Varret, PhD, Michel Krempf, MD, Bertrand Cariou, PhD, Gordan Lauc, PhD, Maryse Guerin, PhD, Alain Carrie, MD PhD, Eric Bruckert, MD PhD, Philippe Giral, MD PhD, Wilfried Le Goff, PhD, Anatol Kontush, PhD*

Sorbonne Université, INSERM, Institute of Cardiometabolism and Nutrition (ICAN), UMR_S1166, F-75013 Paris, France. (Drs Darabi, Guillas, Poupel, Carrie, Bittar, Guerin, Le Goff, and Kontush)

LPS-BioSciences, Université de Paris-Saclay, Orsay, France (Current affiliation of Dr Darabi)

ICAN Analytics, Lipidomics Core, Foundation for Innovation in Cardiometabolism and Nutrition (IHU-ICAN, ANR-10-IAHU-05), Paris, France (Dr Lhomme)

ICAN I/O, Foundation for Innovation in Cardiometabolism and Nutrition (IHU-ICAN, ANR-10-IAHU-05), Paris, France (Dr Ponnaiah)

Department of Metabolic Biochemistry, Pitié-Salpêtrière-Charles Foix Hospital, AP-HP, Paris, France (Drs Bittar and Bonnefont-Rousselot)

Université de Paris, CNRS, INSERM, UTCBS, F-75006 Paris, France (Dr Bonnefont-Rousselot)

Université de Nantes, CHU Nantes, CNRS, INSERM, l'Institut du Thorax, F-44000 Nantes, France (Drs Cariou et Croyal).

Université de Nantes, CHU Nantes, Inserm, CNRS, SFR Santé, Inserm UMS 016, CNRS UMS 3556, F-44000 Nantes, France (Dr Croyal).

CRNH-Ouest Mass Spectrometry Core Facility, F-44000 Nantes, France (Drs Croyal and Krempf).

Paris University and Sorbonne Paris Nord University, National Institute for Health and Medical Research (INSERM, LVTS), F-75018 Paris, France (Dr Varret)

Genos Glycoscience Research Laboratory, Borongajska cesta 83H, HR-10 000 Zagreb, Croatia (Drs Pučić-Baković and Lauc)

Platform MS^3U, Institut de Biologie Paris Seine FR 3631, Sorbonne Université, Paris, France (Dr Matheron)

Department of Haematology, Pitié-Salpêtrière Hospital, Assistance Publique Hôpitaux de Paris, Sorbonne Université, Paris, France (Dr Frere)

Clinique Bretéché, Groupe Elsan, Nantes, France (Dr Krempf)

Endocrinologie Métabolisme et Prévention Cardiovasculaire, Institut E3M et IHU Cardiométabolique (ICAN), Hôpital Pitié Salpêtrière, Paris, France (Drs Bruckert and Giral)

*** Address correspondence to:** Anatol Kontush, PhD, INSERM UMR-S 1166 ICAN, Sorbonne University, Pitié-Salpêtrière 91, boulevard de l'Hôpital, 75013 Paris, France. E-mail anatol.kontush@sorbonne-universite.fr. Tel. (33) (1) 40 77 96 33- Fax. (33) (1) 40 77 96 45

Total number of figures and tables: 6

Nonstandard abbreviations and acronyms: PCSK9, Proprotein Convertase Subtilisin Kexin type 9; ApoA-I, apolipoprotein A-I; HDL, high-density lipoprotein; HDL-C, HDL-cholesterol; LC-MS/MS, liquid chromatography tandem mass spectrometry; SR-BI, scavenger receptor class B type I.

Highlights:

- PCSK9 GOF genetic variants deleteriously affected several metrics of HDL functionality.
- Proteomic, glycomic and lipidomic composition of HDL was altered.
- HDL from FH-PCSK9 patients was enriched in several lysophospholipids.
- A2G2S2 glycan and apolipoprotein A-IV were enriched in HDL from FH-PCSK9 patients.
- A novel mosaic structure-function model of HDL in FH was developed using network analysis.

ABSTRACT

Background: The role of proprotein convertase subtilisin/kexin type 9 (PCSK9) in dyslipidemia may go beyond its immediate effects on low-density lipoprotein receptor (LDL-R) activity.

Objective: This study aimed to assess PCSK9-derived alterations of high-density lipoprotein (HDL) physiology, which bear a potential to contribute to cardiovascular risk profile.

Methods: HDL was isolated from 33 patients with familial autosomal dominant hypercholesterolemia (FH), including those carrying PCSK9 gain-of-function (GOF) genetic variants (FH-PCSK9, n=11), together with two groups of dyslipidemic patients employed as controls and carrying genetic variants in the LDL-R not treated (ntFH-LDLR, n=11) and treated (tFH-LDLR, n=11) with statins, and 11 normolipidemic controls. Biological evaluations paralleled by proteomic, lipidomic and glycomic analyses were applied to characterize functional and compositional properties of HDL.

Results: Multiple deficiencies in the HDL function were identified in the FH-PCSK9 group relative to dyslipidemic FH-LDLR patients and normolipidemic controls, which involved reduced antioxidative, antiapoptotic, anti-thrombotic and anti-inflammatory activities. By contrast, cellular cholesterol efflux capacity of HDL was unchanged. In addition, multiple alterations of the proteomic, lipidomic and glycomic composition of HDL were found in the FH-PCSK9 group. Remarkably, HDLs from FH-PCSK9 patients were systematically enriched in several lysophospholipids as well as in A2G2S2 (GP13) glycan and apolipoprotein A-IV. Based on network analysis of functional and compositional data, a novel mosaic structure-function model of HDL biology involving FH was developed.

Conclusion: Several metrics of anti-atherogenic HDL functionality are altered in FH-PCSK9 patients paralleled by distinct compositional alterations. These data provide a first-ever overview of the impact of GOF PCSK9 genetic variants on structure-function relationships in HDL.

Keywords: proprotein convertase subtilisin kexin type 9, high-density lipoproteins, gain-of-function mutation, low-density lipoprotein receptor, familial hypercholesterolemia, computational biology

Introduction

Proprotein convertase subtilisin/kexin type 9 (PCSK9) is primarily known for its key role in the regulation of low-density lipoprotein (LDL) metabolism through hepatic degradation of the LDL receptor (LDLR) [1]. PCSK9 may however contribute to lipoprotein metabolism in a number of other ways beyond its immediate effects on LDLR activity and LDL-cholesterol (LDL-C) levels [2]. Atherogenic dyslipidemia represents an imbalance between excess circulating levels of cholesterol in the form of apolipoprotein (apo) B-containing relative to apo A-I-containing lipoproteins, which primarily involve LDL and high-density lipoprotein (HDL) respectively [3]. Further understanding of the role of PCSK9 in dyslipidemia and atherosclerosis therefore requires more attention to the modulation of other, than LDL, lipoproteins. While numerous studies characterized associations between PCSK9 and LDL metabolism [4–8], little attention was devoted to relationships of PCSK9 with high-density lipoprotein (HDL). Interestingly, genetic variants of PCSK9 gene and inhibition of classical protein convertases influence HDL-cholesterol (HDL-C) levels [9–11], consistent with a link between PCSK9 and HDL metabolism. Alterations of the metabolism of large, apoE-containing HDL might represent one of the mechanisms underlying this association [10]. This possibility is supported by a physical association of PSCK9 with apoE-containing HDL [12]. Indeed, plasma PCSK9 is carried by both LDL and HDL [13–14].

Low HDL-C level is an independent risk factor for cardiovascular disease; this association may reflect atheroprotective activities of HDL [15]. Indeed, Mendelian randomization reveals that HDL-C is not causally related to cardiovascular disease [16]. Structural and functional differences across HDL particles might therefore be of relevance for the atherogenic role of low HDL-C. Recent compositional and functional data identify several molecular constituents as bioactive components of HDL [17–19]. Notably, HDL subpopulations from patients with acute myocardial infarction and inherited apo-A-I deficiency display altered lipidome and proteome, reflecting impaired function [20, 21]. Importantly, both homozygous and heterozygous familial autosomal dominant hypercholesterolemia (FH) equally features compositionally altered HDL particles exhibiting attenuated functional activity as reported by us [22–24] .

Rare gain-of-function (GOF) genetic variants in PCSK9 lead to a phenotype characteristic of FH [6]. Despite absence of marked effects on plasma HDL-C levels [2, 25, 26], these variants may modulate HDL function. Indeed, PCSK9 decreases the capacity of HDL to reduce oxidative stress in endothelial cells [14], while PCSK9 inhibition increases the capacity of HDL to efflux cellular cholesterol [27] and improves HDL particle profile [28]. In the present study, we explored the role of PCSK9 for the metabolism, composition and function of HDL in humans. We applied state-of-the-art technologies, including multiple

functional evaluations paralleled by proteomic, lipidomic and glycomic approaches, for profiling structure-function relationships across HDL. This strategy allowed us developing a novel structure-function model for the assessment of the HDL biology in relationship to PCSK9. Our data revealed for the first time that HDL particles from PCSK9 patients are less effective in inhibiting oxidative damage, platelet aggregation, inflammatory alterations and apoptosis relative to dyslipidemic and normolipidemic controls. Importantly, multiple alterations of the lipidomics, glycomics, and proteomics of HDL were identified in the patients with genetic variants in PCSK9.

Material and Methods

Patients and samples

For this case-control study, eleven FH patients carrying GOF genetic variants in PCSK9 that reduce cellular levels of LDLR were recruited (FH-PCSK9 group; Figure 1). According to the FH treatment guidelines, all the patients were under statin therapy. The patients were compared to normolipidemic controls (n = 11) as well as to FH patients carrying one of the most common genetic variants in LDLR (FH-LDLR). In order to evaluate the role of the statin treatment, FH-LDLR patients either treated (tFH-LDLR, n = 11) or not treated (ntFH-LDLR, n = 11) by statins were recruited as dyslipidemic controls. The starting dose of a statin varied from 10 to 80 mg/d according to baseline LDL-C levels and was titrated up for patients not reaching their LDL-C goals (<100 mg/dl; 2.6 mmol/l), eventually followed by reduced doses after subsequent check-up. The dyslipidemic FH-LDLR patients were similar to other groups in terms of their biological and clinical characterisitcs, except for gender (Figure 1). In addition to statins, 18 and 45% of the patients in the FH-PCSK9 and tFH-LDLR group, respectively, were under fibrates. No differences in biological and clinical characteristics between patients treated and not treated by fibrates were observed (data not shown). All the patients were admitted to the Department of Endocrinology and Metabolism at the Hospital Pitié-Salpêtrière and Bichat in Paris, or Department of Endocrinology, Metabolic Disease and Nutrition at the Hospital Nord-Laënnec in Nantes, France between 1996 and 2014. No correlation was found between plasma storage time at -80°C and outcome of HDL functionality assays (data not shown).

The exclusion criteria were Type 1 or Type 2 diabetes mellitus (defined as HbA1c >6.5%), endocrine and oncological disease, plasma triglyceride levels >400 mg/dl (4.52 mmol/l), heavy alcohol consumption (>25 g/d), smoking, receiving antioxidative vitamins, evidence of secondary hyperlipidemia (as in nephrotic syndrome), renal insufficiency (creatinine levels >

2.0 mg/dl), and receiving other, than statins, lipid-lowering drugs. The study protocols were approved by the local ethical committees and all subjects provided written informed consent.

Genetic analysis

DNA was extracted from peripheral blood leucocytes on a QIAsymphony automation platform or using the FlexiGene DNA kit (QIAGEN) according to the manufacturer recommendations. Amplification was performed using Multiplicom ADH MASTR assay v2.0 multiplexing kit (Agilent). Alternatively, libraries were prepared using Ampliseq, a SeqCapEZ Solution-Based Enrichment strategy (Roche NimbleGen Madison, WI). Sequencing was performed on coding DNA sequence and flanking introns (exon padding +/- 30 bp) to detect the LDLR, PCSK9, APOB and APOE genes and SNPs included in the wPRS as previously described [29–31]. The pathogenicity of the variants was assumed on the basis of existing data on the role of PCSK9 in FH [6, 32, 33].

Plasma lipoprotein isolation

Total HDL was isolated from 0.8 to 1 mL plasma samples by sequential ultracentrifugation using a table-top ultracentrifuge (Beckmann Optima MAX-XP, CA, USA) and solid KBr for density adjustment [34]. All the samples were thawed only once directly before analysis.

Subfractions of HDL, including HDL2b, d 1.063–1.091 g/ml; HDL2a, d 1.091–1.110 g/ml; HDL3a, d 1.110–1.133 g/ml; HDL3b, d 1.133–1.156 g/ml; and HDL3c, d 1.156–1.179 g/ml, were isolated from 3 ml of plasma by density gradient ultracentrifugation by a slight modification of the method of Chapman et al [35] as previously described [36]. Because of the limited plasma volume, HDL subfractions could not be isolated from subjects in the ntFH-LDLR group, while in the other groups such isolation was possible for three specimens per group only. LDL was isolated from healthy normolipidemic subjects at a density of 1.019-1.063 g/ml by sequential ultracentrifugation. All HDL and LDL particles were extensively dialysed at 4°C in the dark against phosphate-buffered saline (PBS).

Plasma enzyme activity assays

Plasma activities of cholesteryl ester transfer protein (CETP), phospholipid transfer protein (PLTP), and lecithin–cholesterol acyltransferase (LCAT) were measured using fluorescence-based assay kits (Roar Biomedical, Inc., NY, USA) with a fluorescence spectrophotometer (Spectramax Gemini XS, Molecular Devices, CA, USA). These measurements were carried out following the manufacturer's instruction as previously described [37]. In brief, for CETP activity assay, 4 μl of plasma sample (as the source of CETP) was added to the reaction mixture containing a synthetic fluorescent cholesteryl ester (CE) in a self-quenched state as

the donor molecule and apo-B-containing lipoprotein as an acceptor particle. The increase in fluorescence intensity was quantified at excitation wavelength of 465 nm and emission wavelength of 535 nm as the CETP-mediated transfer of the fluorescent neutral lipid to the acceptor particle and expressed as nanomole of neutral lipid transferred per µl plasma per hour.

Based on the same principle, PLTP activity was measured using a fluorescent phospholipid donor and a synthetic acceptor, in the presence of 3 µl of plasma as a source of PLTP. The transfer was characterised by an increase in fluorescence intensity, which was read at excitation wavelength of 465 nm and emission wavelength of 535 nm.

For LCAT, 4 µl of plasma was added to the assay substrate and 96 µl of the assay buffer. After 2.5h incubation at 37°C, 200 µl of the read reagent was added to the mixture and following the transfer of 200 µl of the mixture to a black fluorescent plate, fluorescence was read at excitation wavelength of 340 nm and two distinct emissions wavelengths of 470 nm and 390 nm, corresponding to non-hydrolyzed and hydrolyzed phosphatidylcholine, respectively. Results were reported as the ratio of the fluorescence of the hydrolyzed and non-hydrolyzed substrate.

Antithrombotic activity of HDL

Fresh blood was collected into 3.8% trisodium citrate as an anticoagulant. Platelet-rich plasma (PRP) was prepared by centrifugation at 100g for 20 minutes at 22°C. To prevent platelet activation, PRP was acidified at pH 6.4. Following platelet separation by centrifugation, platelet pellets were gently resuspended in Tyrode buffer (137 mM NaCl, 12 mM $NaHCO_3$, and 2.5 mM KCl [pH 7.2]). The concentration was adjusted accordingly with Tyrode buffer. To measure HDL-mediated antithrombotic effects, platelets were preincubated with HDL 50µg protein/ml for 5 minutes at 37°C with stirring at 1000 rpm. Collagen (10µg/ml) was used as an agonist and aggregation was monitored for 4 min using a Lumi-aggregometer type 500 VS (Chrono-log) [38].

Antiapoptotic activity of HDL

The capacity of HDL to protect against starvation-induced apoptosis was measured in human umbilical vein endothelial cells (HUVECs). The cells (5×10^5 cells/mL) were cultured for 24h in 24-well plates using an endothelial cell growth media (PromoCell, Germany) containing all required growth factors and supplements. To induce quiescence, HUVEC cells were maintained overnight in the basal medium with 0.5% serum growth supplement. Subsequently, the cells were washed twice with PBS to remove growth factors. Deprived cells were then incubated in the presence or absence of HDL (100 µg protein/mL) for 16h.

Annexin V-FITC kit (BioLegend, CA, USA) was used to evaluate cellular apoptosis and necrosis as described previously [39]. Flow cytometric measurements were performed on a BD LSRFortessa flow cytometer (BD Biosciences, NJ).

Antioxidative activity of HDL toward LDL oxidation

Antioxidative function of HDL during LDL oxidation was characterized as previously described [23, 40]. Native LDL (d1.019 –1.063 g/L) isolated from a healthy normolipidemic donor was added, at a concentration of 10 mg cholesterol/dl, to PBS alone or total HDL (40 mg total mass/dl) followed by the addition of 2,2′-azobis 2-methylpropionamidine dihydrochloride (AAPH,1 mM), an azo-initiator of oxidation. Kinetics of LDL oxidation was followed for 16 h at 37°C as the increment in absorbance at 234 nm corresponding to the accumulation of conjugated dienes as compared to the blank containing AAPH alone. The kinetics of conjugated diene accumulation identified two characteristic phases, the lag and propagation phases. For each kinetic curve, the oxidation rate in the lag and propagation phase and the maximal amount of conjugated dienes were calculated and the results were expressed as a percentage relative to LDL oxidized in the absence of HDL [41].

Cholesterol efflux capacity of HDL

The capacity of HDL to efflux cellular cholesterol was evaluated as previously described [17, 42]. Human monocyte-derived THP-1 cells were cultured in RPMI 1640, and PMA was used to differentiate the cells into macrophages. After incubation with acetylated LDL (50 μg/mL) and ^{3}H-cholesterol (1 μCi/mL) for 48 h, washed cells were incubated with HDL. After 4 h the radioactivity of the supernatant and lysed cells was determined by liquid scintillation counting. The percentage of cholesterol efflux was calculated as the percentage of counts recovered from the medium divided by total counts present on the plate (medium + cells) [17].

Cell-free anti-inflammatory activity of HDL

The anti-inflammatory capacity of HDL was measured using an in vitro cell-free method [23]. In brief, reference LDL isolated from a healthy normolipidemic subject (50 μg protein/ml ≈ 0.1 μM) was incubated in PBS with either dichlorofluorescine (DCFH) alone or with a mixture of DCFH and HDL (50 μg protein/ml ≈ 0.35 μM). DCFH is a non-fluorescent probe that upon interaction with lipid oxidation products, such as oxidized phospholipids, forms DCF, which produces intense fluorescence [43]. To initiate mild LDL oxidation, copper sulfate at a final concentration of 0.05 μM Cu^{2+} was added and the kinetic of oxidation was determined by monitoring the change in the DCF fluorescence at every 5 min interval at 37°C for 16 h, at

excitation wavelength of 485 nm and emission wavelength of 528 nm using a florescence spectrophotometer [23].

Lipidomic analysis

HDL samples from different study groups were randomized and lipids were extracted using a modified Bligh and Dyer method as previously described [44]. Samples (30 μg HDL phospholipid (PL)) were supplemented with a mixture of internal standards (Avanti Polar Lipids, Alabaster, AL) and extracted with 1,2 ml methanol/$CHCl_3$ (2:1 v/v) in the presence of butylated hydroxytoluene and 310 μl of 0,005 N HCL. Phase separation was triggered by adding of 400μl $CHCl_3$ and 400μl H_2O. Extracted lipids were dried and resuspended in liquid chromatography-tandem mass spectrometry (LC/MS/MS) solvent. Blanks (one every 15 samples), quality controls (one every 5 samples) and an additional pool quality control containing equal amounts of all the samples (injected every 15 samples) were extracted in parallel to ensure data integrity.

Lipids were quantified using LC-MS/MS with a Prominence UFLC (Shimadzu, Tokyo, Japan) and QTrap 4000 mass spectrometer (AB Sciex, Framingham, MA, USA). Eight major PL subclasses were quantified, including phosphatidylcholine (PC), lysophosphatidylcholine (LPC), phosphatidylethanolamine (PE), lysophosphatidylethanolamine (LPE), phosphatidylinositol (PI), phosphatidylglycerol (PG), phosphatidylserine (PS), and phosphatidic acid (PA), two principal sphingolipid (SL) subclasses, including sphingomyelin (SM) and ceramide (Cer), and one neutral lipid subclass, triglycerides (TG), which together comprised 222 individual molecular lipid species. Samples were injected on to a Kinetex HILIC 2.6μm 2.1x150mm column (Phenomenex, CA, USA). Mobile phases consisted of (A) 30mM ammonium acetate and 0.2% acetic acid and (B) acetonitrile containing 0.2% acetic acid. Lipid species were detected in positive ionisation mode using scheduled multiple reaction monitoring (sMRM) reflecting their head group fragmentation for PL and SM, sphingoid base fragmentation for ceramides and neutral loss of single acyl chain for TG. The nomenclature used for TG is therefore TG (a:b_c:d) where a:b corresponds to the fragmented chain and c:d to the sum of both remaining chains. Quantification was performed using calibration curves specific for the 11 individual lipid classes with up to 12 component fatty acid moieties per class. More abundant lipid species which displayed non-linear response in non-diluted extracts (typically PC and some SM species) were quantified from a 100-fold diluted sample. sMRM signals were corrected for isotopic contribution using an in-house developed R script adapted from Ejsing CS et al [32].

Proteomic analysis

Prior to protein digestion, samples were dialyzed overnight against 100 mM ammonium bicarbonate. Isolated HDLs were diluted in a buffer containing a mixture of ammonium bicarbonate and urea (50 mM and 4 M, respectively). Following reduction of cysteine residue with dithiothreitol (DTT, 2.3 mM) at 56°C for 30 min and alkylation with iodoacetamide (5 mM) at room temperature for 30 min, dithiothreitol was added to the samples at a final concentration of 2.3 mM.

The mixtures were diluted 2-fold with 50 mM ammonium bicarbonate, and digestions were carried out at 37°C overnight in the presence of trypsin at a 1:30 protein/enzyme ratio. Digestion was stopped by acidification with 5% formic acid. Samples were desalted in Sep-Pak C18 cartridges (Waters, Milford, MA, USA) using acetonitrile / 2% formic acid for elution. Subsequently, one µg of protein digest mixed with glutamate dehydrogenase digest (LaserBio Labs, Sophia-Antipolis, France) were analyzed on a chromatography system (nano-LC Ultimate 3000; Dionex, Amsterdam, The Netherlands) and loaded onto trapping column C18 (5 µm, 10 nm pore, 300 µm i.d., LC Packings, France) at a flow rate of 20 µl/min for 10 min and eluted using solvent A (2% acetonitrile and 0.1% formic acid in H_2O). Following separation on a 50 cm analytical column packed with C18 phase (3 µm, 75 µm i.d.) at 300 nL/min, samples were resolved using gradient of solvent B as follows: 1% solvent B (98% acetonitrile, 0.1% formic acid) to 40% B in 60 min, 40% B to 60% B in 2 min, 60% B for 8 min [45].

Glycomic analysis

HDL samples were desalted with ice-cold methanol as previously described [46, 47] and dried in a vacuum concentrator. Samples were then resolved and incubated in 30 µl of sodium dodecyl sulfate (1.33%) for 10 min at 65°C for protein denaturation. Samples were further treated with Igepal CA-630 (Sigma-Aldrich, St. Louis, MO, USA) prior to overnight incubation at 37°C with 2.4 U of PNGase F (10 U/µL, Promega, Madison, WI, USA). Next, a two-step fluorescent labelling method was used to label N-glycans with procainamide hydrochloride dye (ProA, Acros Organics) upon their release. To remove remaining free labels and reducing agents, hydrophilic interaction liquid chromatography solid-phase extraction (HILIC-SPE) was used as described earlier [46, 47]. Selective separation of glycans was achieved by liquid chromatography with fluorescence detection (HILIC-UHPLC-FLD) on a Waters Acquity UHPLC H-Class system (Milford, MA, USA). Briefly, separation was performed on Waters BEH Glycan chromatography column (150×2.1mm i.d., 1.7 µm BEH particles). Phase A and B contained ammonium formate (100 mM) and acetonitrile, respectively, and a linear gradient of 70–53% acetonitrile (v/v) at a flow rate of 0.56 ml/min was used in a 23 min analytical run. The detection of labeled glycans was performed at excitation wavelength of 310 nm and emission wavelength of 370 nm. The obtained

chromatograms were separated in the same manner into 23 chromatographic peaks and the abundance of glycans in each peak was expressed as % of total integrated area. Following their separation, glycans were annotated according to measured *m/z* value and recorded fragmentation spectra obtained by Bruker Compact Q-Time-of-Flight mass spectrometer coupled to UHPLC via Ion Booster ion source and controlled using HyStar software (Bruker Daltonics, Bremen, Germany). Spectra were analyzed using Bruker Data analysis software version 4.4, while glycan composition and certain structural features were determind using GlycoMod [48] and GlycoWorkbench [49] software tools were used.

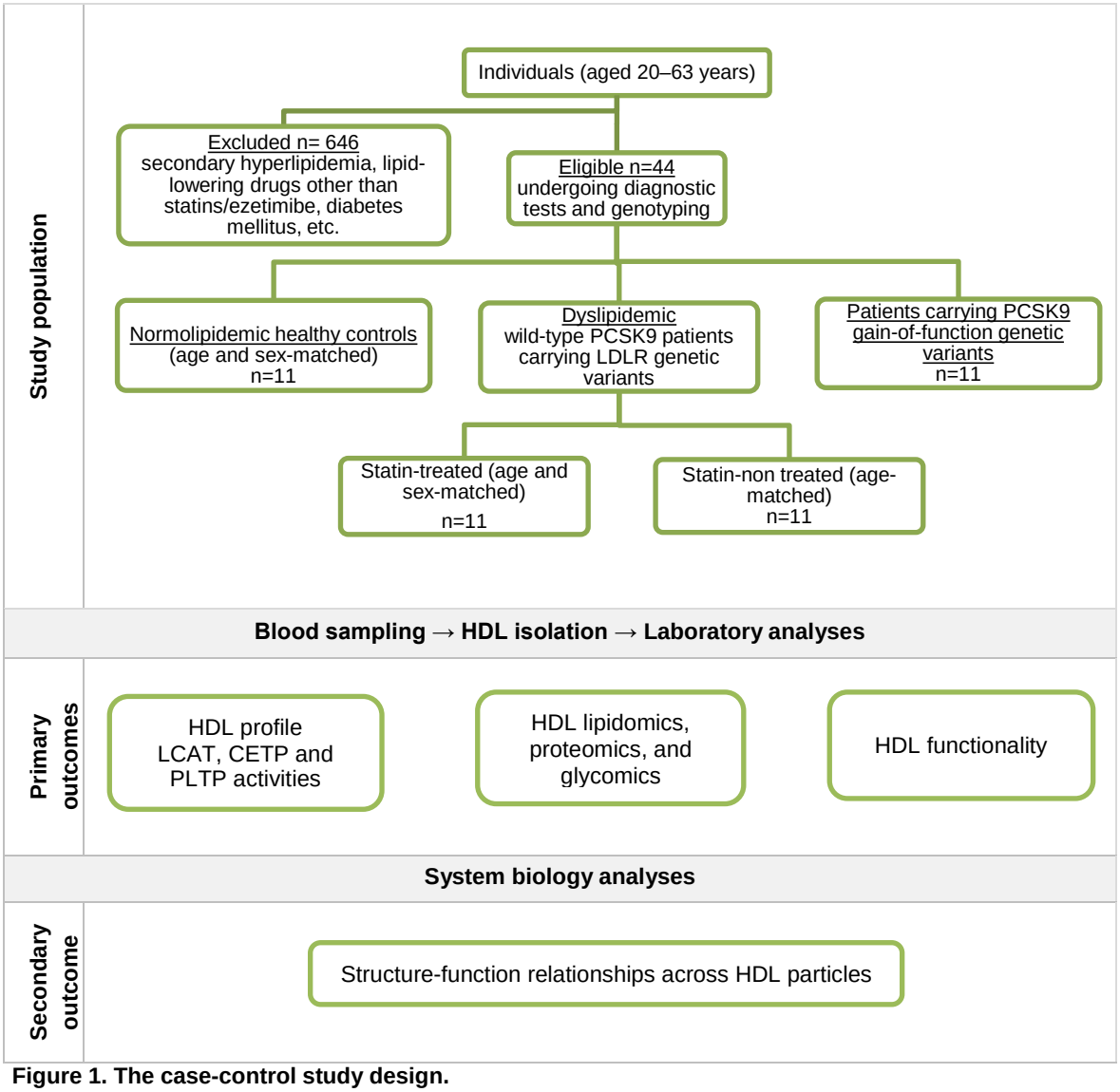

Figure 1. The case-control study design.

Statistical analyses

Distributions of all variables were analyzed for normality using the D'Agostino-Pearson test. One-way ANOVA with post-hoc Tukey or Kruskal-Wallis with post-hoc Dunn's test were

employed to compare groups with normal or non-normal distributions, respectively. Fisher's exact test was used to compare categorical variables between the groups. Structure-function relationships across HDL particles were elucidated using systems biology approaches involving cluster and network analyses. All the features that were significant in each of the omics analysis, including lipidomic, glycomic, proteomic, biological and functional parameters, were used to calculate the correlation coefficients between all these variables. A correlation network was constructed using Cytoscape (version 3.7.0) [50] plug-in Metscape (version 3.1.3) [51] and clustered by tree layout. Since multiple omics measurements were performed in a relatively small population of subjects, rigorous corrections for multiple comparison were made to eliminate Type 1 errors according to Benjamini-Hochberg [52]. Between-assay variability (potentially resulting in Type 2 errors) in omics data was corrected by including a reference sample in each batch of studied samples. After removing outliers, false discovery rate (FDR) multiple testing correction was performed on variables that passed the cut-off of $p < 0.05$.

Results

Characteristics of subjects

Main clinical and biological characteristics of the subjects are shown in Table 1. The groups did not differ in age, sex ratio and BMI. As expected, LDL-C concentrations were elevated in FH-PCSK9 patients relative to normolipidemic controls (+88%, $p = 0.024$) but not relative to ntFH-LDLR and tFH-LDLR patients who both displayed increased LDL-C as compared to normolipidemic controls. Such cholesterolemia was expectedly more pronounced in non-treated than treated FH-LDLR patients (+153%, $p < 0.0001$, vs. +86%, $p = 0.0018$, respectively). As a result, both FH-PCSK9 and tFH-LDLR groups revealed reduced levels of LDL-C as compared to ntFH-LDLR patients (-26%, $p < 0.0012$, and -27%, $p = 0.018$, respectively).

HDL-C concentrations tended to be decreased in both FH-PCSK9 and FH-LDLR patients relative to normolipidemic controls, while TG levels tended to be increased (+10 to +90%, $p > 0.05$). Moreover, TGs were significantly elevated in FH-PCSK9 patients vs. normolipidemic subjects (+91%, $p = 0.04$). Finally, both FH-PCSK9 and FH-LDLR patients showed significant elevation in plasma total cholesterol (TC) as compared to normolipidemic subjects (> +75%, $p < 0.01$).

The ratio of TC to HDL-C was significantly elevated in FH-PCSK9 patients relative to normolipidemic controls (+113%, $p = 0.0006$). While plasma PLTP activity was significantly attenuated in both FH-PCSK9 and FH-LDLR patients as compared to normolipidemic controls (-22 to -28%, $p < 0.05$), similar trend for the LCAT activity only reached significance

in ntFH-LDLR patients (-10%, $p < 0.03$). Plasma CETP activity showed no significant differences among the groups.

Chemical composition of HDL particles

HDL tended to show enrichment in CE in FH-PCSK9 (+26%, $p = 0.093$), tFH-LDLR (+28%, $p = 0.059$) and ntFH-LDLR (+31% $p = 0.025$) groups relative to normolipidemic HDL (Table 2). By contrast, free cholesterol (FC) content of HDL from FH-PCSK9 patients, ntFH-LDLR and tFH-LDLR tended to be reduced (-35%, $p = 0.14$; -38%, $p = 0.037$; -29%, $p = 0.33$; respectively). Similarly, PL was depleted in FH HDL relative to normolipidemic HDL as follows: FH-PCSK9, -17%, ($p = 0.020$), ntFH-LDLR, -27%, ($p = 0.003$) and tFH-LDLR, -34%, ($p = 0.48$; Table 2). By contrast, no difference in the TG and total protein content was observed across the groups. Consistent with these data, analysis of HDL subfractions showed that CE content of FH HDL particles was elevated while their PL content was reduced compared to their counterparts from normolipidemic controls (Supplementary Table 1).

Antiapoptotic and antithrombotic activity of HDL

Endothelial antiapoptotic effects of FH-PCSK9 (-15%, $p < 0.0001$) were inferior to that of normolipidemic HDL upon starvation (-41%, $p < 0.0001$). While there was no difference between the three FH groups, the antiapoptotic effects of normolipidemic HDL were superior to those of HDL from the ntFH-LDLR and tFH-LDL-R groups (-41%, $p < 0.0001$; -18%, $p = 0.001$; -11%, $p < 0.0001$ respectively; Figure 2A).

While FH-PCSK9 and ntFH-LDLR HDLs were without effect, platelet aggregation was efficiently inhibited by HDL from the normolipidemic and tFH-LDLR groups (-22%, $p = 0.007$; and -17%, $p = 0.049$ respectively; Figure 2B). However, FH-PCSK9 HDL showed no difference from the other groups with respect to the antithrombotic activity.

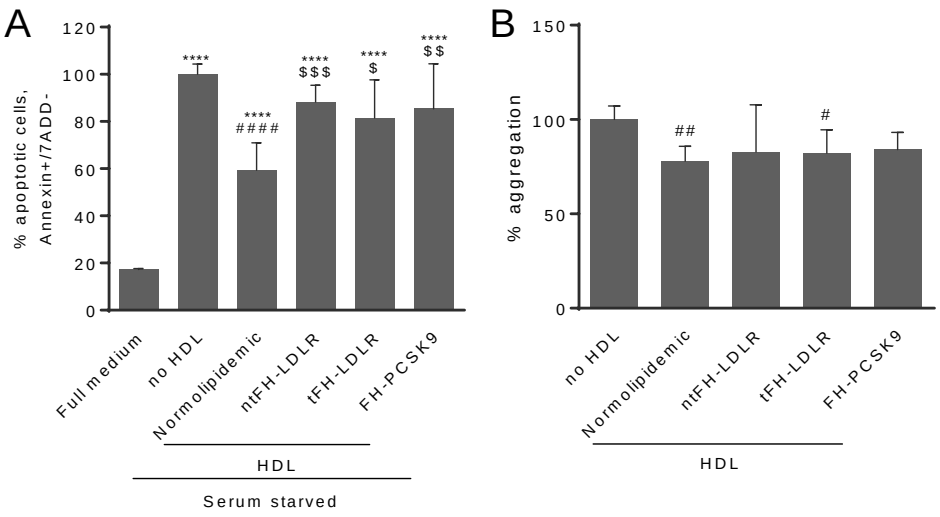

Figure 2. Effect of HDL from patients with gain-of-function PCSK9 genetic variants (FH-PCSK9) as well as from normolipidemic controls and patients carrying genetic variants in LDL receptor non treated (ntFH-LDLR) and treated with a statin (tFH-LDLR). (A) Cells were cultured under serum deprivation in the absence or presence of HDL at 100 µg protein/ml for 16 h. The percentage of apoptotic cell death was determined by flow cytometry using annexin V. (B) Platelets from healthy subjects were incubated in the absence or presence of HDL at 50 µg protein/ml for 10 min at 37°C following stimulation with collagen (0.24-0.31 µg/ml). Data are shown as means ± SD (n ≥ 11 per group); * vs. reference full medium; $^{\#}$ vs. non-treated cells; $^{\$}$ vs. normolipidemic HDL. Single, double, triple, and quadruple symbols indicate p< 0.05, 0.01, 0.001, and 0.0001, respectively.

Antioxidative activity of HDL

While FH-PCSK9 HDL was inefficient, HDL from normolipidemic (-52%, p = 0.0001), ntFH-LDLR (-24%, p = 0.036) and tFH-LDLR (-30%, p = 0.0024) groups significantly decreased LDL oxidation rate in the propagation phase as compared to LDL oxidised alone, (Figure 3A). Furthermore, all HDLs, except that from the FH-PCSK9 group, significantly reduced maximal diene formation as compared to LDL alone (<-15%, p < 0.01; Figure 3B). In addition, LDL oxidation rate in the presence of HDL from the FH-PCSK9 (+64%, p = 0.0018) and ntFH-LDLR (+59%, p = 0.013) groups was elevated as compared to that measured in the presence of HDL from the normolipidemic group. Similarly, HDL from the normolipidemic group showed more potent activity in attenuation maximal diene formation as compared to HDL from FH groups (>-12%, p < 0.001).

Cholesterol efflux capacity

No significant difference was observed in cholesterol efflux capacity of HDL from lipid-loaded THP-1 macrophages between patients carrying genetic variants resulting in FH and normolipidemic controls (Figure 3C).

Cell-free anti-inflammatory activity

HDL modulates inflammatory response both directly via endothelial adhesion molecule expression and indirectly by protecting LDL from generation of proinflammatory lipids upon oxidation. The latter property of HDL was employed to develop a cell-free functional assay, which measures the ability of HDL to prevent accumulation of proinflammatory oxidised phospholipids (oxPL) in a cell-free 2',7'-dichlorofluoresceine (DCF)-based assay in the presence of Cu^{2+} to induce oxidation. All HDLs showed a tendency to inhibit Cu^{2+}-induced accumulation of oxPL in LDL (<-80%; Figure 3C). Nevertheless, elevated levels of oxPL were observed in the presence of HDL from the FH-PCSK9 (+182%, p = 0.021) and ntFH-LDLR (+251%, p = 0.003) groups relative to those measured with HDL from normolipidemic controls (Figure 3D), indicative of deficient antiinflammatory capacity of FH HDL.

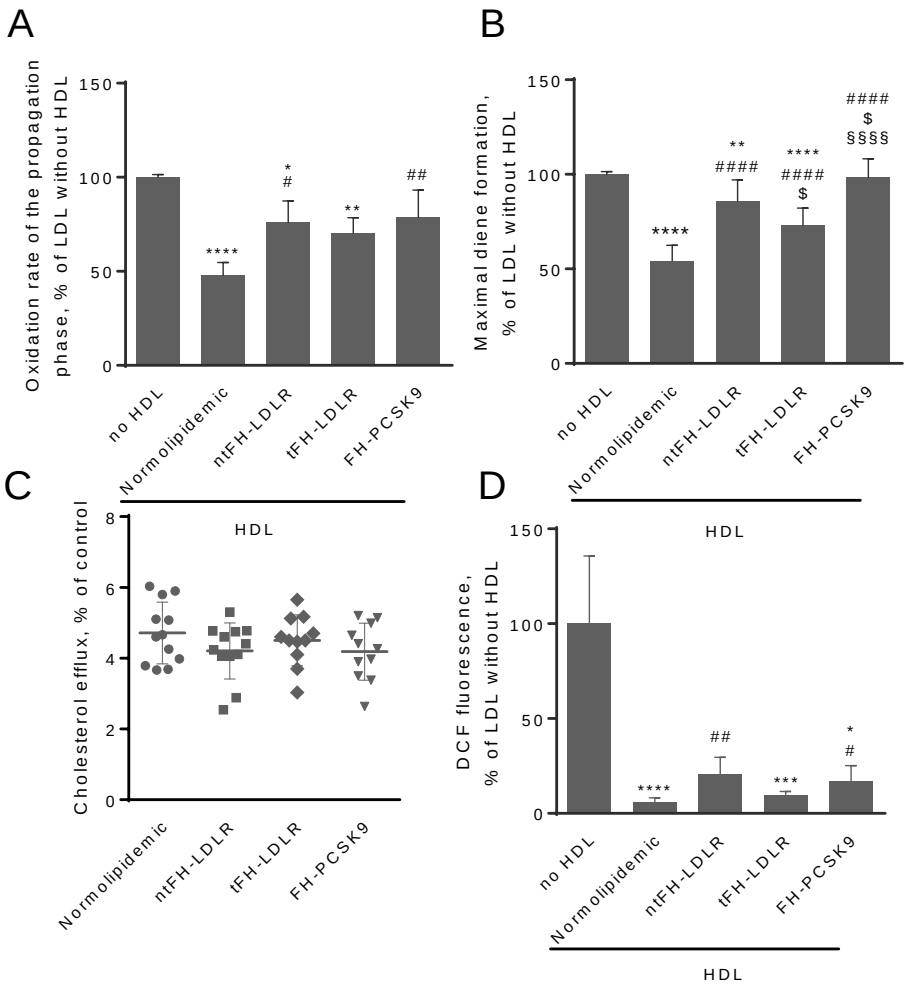

Figure 3. Antioxidative activity, cholesterol efflux capacity and cell-free anti-inflammatory activity of HDL from patients with gain-of-function PCSK9 genetic variants (FH-PCSK9) as well as from normolipidemic group and patients carrying genetic variants in LDL receptor not treated (ntFH-LDLR) and treated with statin (tFH-LDLR). (A) Influence of HDL (40 mg total mass/dL) on the LDL oxidation rate in the propagation

phase and (B) maximal diene formation during 2,2'-azobis-(2-amidinopropane) hydrochloride (AAPH)-induced oxidation of reference LDL (10 mg TC/dL; AAPH,1 mM). LDL was oxidized in phosphate-buffered saline (PBS) at 37°C and conjugated diene formation was measured by absorbance increment at 234 nm. (C) Cellular [^{3}H]-cholesterol efflux from macrophages to HDLs was initially calculated as the percentage amount of the label recovered in the medium divided by the total label in each well. (D) Cell-free anti-inflammatory activity of HDLs assessed as inhibition of Cu^{2+}-induced formation of proinflammatory oxPL. The potency of HDL (20 mg total mass/dL) against Cu^{2+}-induced accumulation of oxPL in reference LDL (LDL, 5 mg TC/dL; Cu^{2+}, 0.05μM) as reflected by DCF fluorescence was evaluated. LDL was oxidized in PBS at 37°C, and the fluorescence intensity of DCF (0.2 mg/ml) was measured over 24 h at 485/530 nm. Data are shown as % fluorescence intensity of DCF measured in reference LDL incubated without added HDL. Data are shown as means ± SD (n ≥ 10). * vs. reference LDL alone (incubated without added HDL); $^{\#}$ vs. normolipidemic; $^{\$}$ vs. ntFH-LDLR, and § vs. tFH-LDLR. Single, double, triple, and quadruple symbols indicate p< 0.05, 0.01, 0.001, and 0.0001, respectively.

Omics

A total of 63 protein, 23 carbohydrate and 222 lipid species were detected in HDL particles using targeted mass spectrometry. FH-PCSK9 HDL showed enrichment in 22 individual proteins relative to normolipidemic HDL, of which only apoA-IV, α-1-acid glycoprotein 2, platelet basic protein, serotransferrin and haptoglobin were equally enriched in HDLs from FH-LDLR patients employed as dyslipidemic controls (Supplementary Figure 1, A and B and Supplementary Figure 2). Enrichment in two proteins, including Ig gamma-1 chain C region and Ig lambda-6 chain C region, was specific for FH-PCSK9 HDL. ntFH-LDLR HDLs showed significant alterations in 26 protein species relative to normolipidemic subjects, while only 16 individual proteins were altered in the tFH-LDLR HDL (Supplementary Figure 1, B), consistent with a partial normalization of the proteome by the treatment. Interestingly, most of these 16 proteins, including complement C3, apoA-IV, haptoglobin, apoCII, transthyretin and serotransferrin, were commonly enriched in HDL from both ntFH-LDLR and tFH-LDLR patients relative to normolipidemic controls, suggesting a treatment-independent effect of FH. In addition, serum amyloid A-1, beta-2-glycoprotein 1 (apoH), and beta-2-microglobulin were depleted in the tFH-LDLR vs. ntFH-LDLR HDL, indicative of the treatment effect (data not shown).

For 23 glycan peaks (GPs) identified in HDL particles (Supplementary Table 2 and Supplementary Figure 3), there was no difference in the glycomic composition of HDL between FH-PCSK9 and FH-LDLR patients employed as dyslipidemic controls, indicative of the absence of specific effects of PCSK9 genetic variants on the HDL glycome (Supplementary Figure 1, C). Enrichment in GP13 and depletion of GP3, GP12 and GP16 was common for all the three FH groups (Supplementary Figure 1, C and D).

Lipidomic analysis revealed that the FH-PCSK9 group was distinguished from the two FH-LDLR dyslipidemic groups by the HDL content of 42 lipid species, predominantly TGs

(Supplementary Figure 1, E). Among these species, the content of TG (16:0/36:4), TG (14:0/36:4) and TG (18:2/32:2) was also different relative to normolipidemic controls, with all the species being depleted in the FH-PCSK9 HDL. Interestingly, only 11 of 62 altered lipid species were enriched in the FH-PCSK9 HDL as compared to the other groups, while most of the lipids were depleted.

Together, our data showed that when the FH-PCSK9 group was compared to the both dyslipidemic and normolipidemic controls, HDL lipidomics displayed the most pronounced differences and glycomics the least pronounced differences (Supplementary Figures 1, 2 and 4). Consistent with this result, statin treatment, while partially reversing proteomic and glycomic alterations, caused more variation in the HDL lipidome.

Network analysis

Proteomics. Correlations between HDL content of 32 individual proteins were organised into four clusters (Supplementary Figure 5, A). The largest cluster was formed by functionally distinct proteins, including hemopexin, transthyretin and angiotensinogen. Interestingly, abundances of complement C3, platelet basic protein and platelet factor-4 protein were correlated within a single cluster, while those of apolipoproteins, including apo A-II, apo A-IV, apo C-II, apo C-III, apo E and apo F, were clustered separately. Abundances of four other proteins, including serum amyloid A-1, galectin-3-binding protein, haptoglobin and alpha-1-antitrypsin, formed a separate cluster.

*Glycomics. A*bundances in HDL of highly sialylated GPs, including GP12, GP15, GP16 and GP18, were positively correlated with each other but not with that of GP13 (Supplementary Figure 5, B). On the other hand, abundances of non-sialylated GPs, including GP2 and GP3, were positively correlated with each other but not with that of GP1.

Lipidomics. Abundances in HDL of 31 lipid species from various classes, including PA, PI, PE, PC, PG, LPE, LPC, TG, and Cer, revealed strong intercorrelations which were organised into five distinct clusters (Supplementary Figure 5, C). Interestingly, abundances of 22 of these species were identified as features distinguishing FH and normolipidemic control HDLs (Supplementary Figure 1, E and F).

Structure-function analysis. Structure-function relationships across HDL revealed nine distinct clusters (Figure 4, A). The largest cluster was formed by lipids and included 70 lipid species. Proteins were present in several clusters formed either exclusively by proteins themselves or by proteins together with lipids, glycans and functional metrics of HDL. Glycans were present in two clusters only.

Functional metrics revealed complex associations with compositional features of HDL. Indeed, antioxidative activity of HDL formed a cluster with 8 lipid species, 8 glycans and one

protein (transthyretin) as well as with plasma levels of cholesterol, TG and LDL-C (Figure 4, A and B). Antiapoptotic activity of HDL was associated with the abundance of a single lipid species PG (36:3) and with plasma HDL-C, while anti-inflammatory and antithrombotic functions were interrelated but unrelated to HDL composition. Cholesterol efflux capacity of HDL was specifically associated with the abundances of serotransferrin and haptoglobin in HDL as well as with plasma activities of CETP, PLTP and LCAT.

A

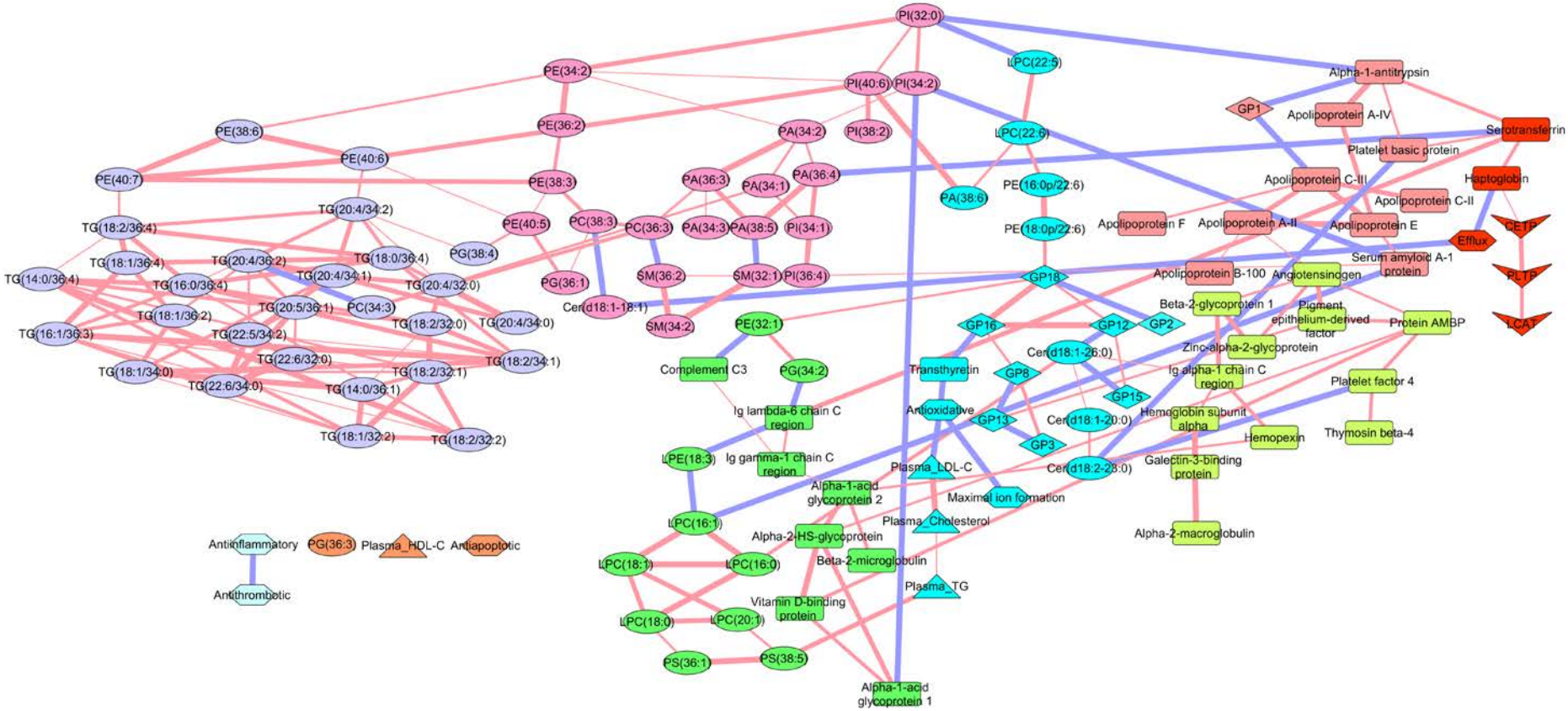
PI(32:0)
PE(34:2)
PI(40:6)
PI(34:2)
LPC(22:5)
PE(36:2)
PA(34:2)
PI(38:2)
LPC(22:6)
PE(38:6)
PE(40:6)
PE(40:7)
PE(38:3)
PA(36:3)
PA(34:1)
PA(36:4)
PA(38:6)
PE(16:0p/22:6)
PE(18:0p/22:6)
TG(20:4/34:2)
TG(18:2/36:4)
PE(40:5)
PC(38:3)
PC(36:3)
PA(34:3)
PA(38:5)
PI(34:1)
TG(18:1/36:4)
TG(20:4/36:2)
TG(18:0/36:4)
PG(38:4)
TG(14:0/36:4)
TG(20:4/34:1)
PG(36:1)
SM(36:2)
SM(32:1)
PI(36:4)
TG(16:0/36:4)
TG(20:4/32:0)
Cer(d18:1-18:1)
TG(20:5/36:1)
PC(34:3)
TG(18:1/36:2)
TG(18:2/32:0)
TG(20:4/34:0)
SM(34:2)
PE(32:1)
TG(16:1/36:3)
TG(22:5/34:2)
TG(22:6/32:0)
TG(18:2/34:1)
TG(18:1/34:0)
Complement C3
PG(34:2)
TG(18:2/32:1)
TG(22:6/34:0)
TG(14:0/36:1)
Ig lambda-6 chain C region
TG(18:1/32:2)
TG(18:2/32:2)
LPE(18:3)
Ig gamma-1 chain C region
LPC(16:1)
LPC(18:1)
LPC(16:0)
LPC(18:0)
LPC(20:1)
PS(36:1)
PS(38:5)
Alpha-1-acid glycoprotein 1
Alpha-1-acid glycoprotein 2
Alpha-2-HS-glycoprotein
Beta-2-microglobulin
Vitamin D-binding protein
Transthyretin
Antioxidative
Plasma_LDL-C
Maximal ion formation
Plasma_Cholesterol
Plasma_TG
GP18
GP16
GP12
GP2
GP8
GP15
GP13
GP3
Cer(d18:1-26:0)
Cer(d18:1-20:0)
Cer(d18:2-28:0)
Alpha-1-antitrypsin
GP1
Apolipoprotein A-IV
Serotransferrin
Platelet basic protein
Apolipoprotein C-III
Haptoglobin
Apolipoprotein C-II
Apolipoprotein F
Apolipoprotein A-II
Apolipoprotein E
CETP
Efflux
PLTP
LCAT
Serum amyloid A-1 protein
Apolipoprotein B-100
Angiotensinogen
Beta-2-glycoprotein 1
Pigment epithelium-derived factor
Protein AMBP
Zinc-alpha-2-glycoprotein
Ig alpha-1 chain C region
Platelet factor 4
Hemoglobin subunit alpha
Hemopexin
Thymosin beta-4
Galectin-3-binding protein
Alpha-2-macroglobulin
Antiinflammatory
PG(36:3)
Plasma_HDL-C
Antiapoptotic
Antithrombotic

B

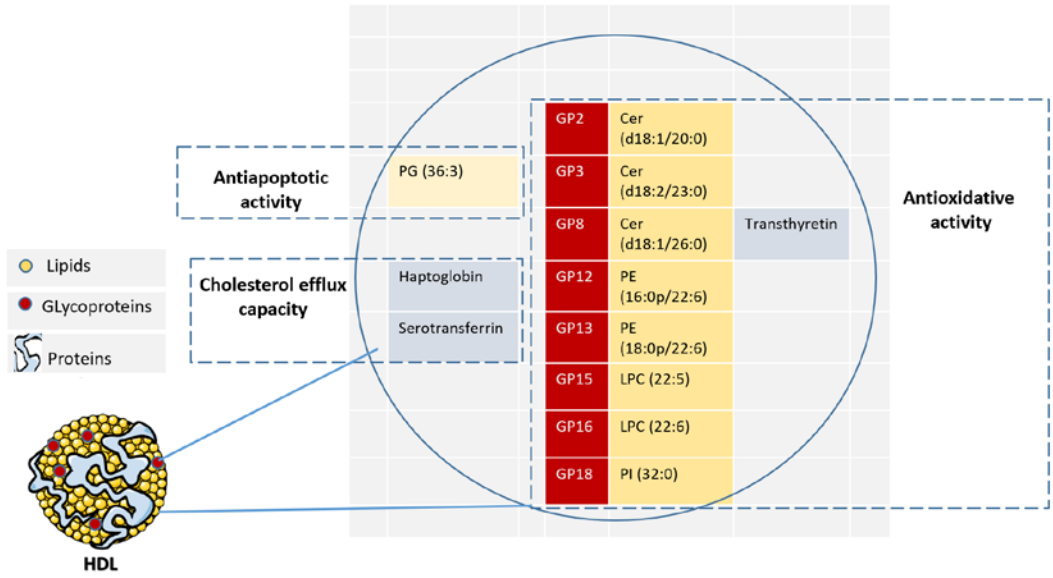

Figure 4. Global network analysis of structure-function relationships across HDL. (A) Global pathway clustering was performed across all studied groups using datasets of HDL proteomics (rectangle) glycomics (diamonds), lipidomics (ovals) and functional metrics (hexagones), together with clinical parameters (triangles). Different colors of nodes correspond to different clusters and edges represent positive (red) or negative (blue) correlations. The thickness of the edge represents the strength of the correlations. **Purple cluster**: PE(38:6), PE(40:6),TG(20:4/34:2), PG(38:4), PE(40:7), TG(18:2/36:4),TG(18:1/36:4), TG(14:0/36:4), TG(20:4/36:2), TG(16:0/36:4), TG(18:1/36:2), TG(16:1/36:3),TG(18:0/36:4), TG(20:4/34:1), TG(20:5/36:1), PC(34:3), TG(22:5/34:2), TG(22:6/32:0), TG(22:6/34:0), TG(18:1/34:0), TG(20:4/32:0), TG(18:2/32:0), TG(20:4/34:0), TG(18:2/34:1), TG(18:2/32:1), TG(14:0/36:1), TG(18:1/32:2), TG(18:2/32:2). **Pink cluster:** PE(34:2), PE(36:2), PE(38:3), PE(40:5), PC(38:3), PG(36:1), Cer (d18:1/18:1), PC(36:3), SM(36:2), SM(34:2), PA(36:3), PA(34:3), PA(38:5), SM(32:1), PA(34:2), PA(34:1), PI(34:1), PI(36:4), PA(36:4), PI(32:0), PI(40:6), PI(34:2), PI(38:2). **Green cluster**: PE(32:1), complement C3, PG(34:2), Ig lambda-6-chain C region, LPE(18:3), Ig gamma-1-chain C region, alpha-1-acid glycoprotein 2, alpha-2-HS glycoprotein, LPC(16:1), LPC(18:1), LPC(16:0), LPC(18:0), LPC(20:1), PS(36:1), PS(38:5), vitamin D-binding protein, Beta-2-macroglobulin, alpha-1-acid glycoprotein 1. **Turquoise cluster**: LPC(22:5), LPC(22:6), PA(38:6), PE(16:0p/22:6), PE(18:0p/22:6), GP18, GP16, GP12, GP8, GP13, GP3, GP2, GP15, transthyretin, antioxidative activity, plasma LDL-C, maximal diene formation, plasma cholesterol, plasma TG, Cer (d18:1/26:0), Cer (d18:1/20:0), Cer (d18:2/23:0). **Light red cluster:** alpha-1-antitrypsin, apolipoprotein A-IV, platelet basic protein, apolipoprotein C-III, apolipoprotein C-II, apolipoprotein E, apolipoprotein A-II, apolipoprotein F, apolipoprotein B-100, serum amyloid A-I protein, GP1. **Red cluster**: serotransferrin, haptoglobin, cholesterol efflux capacity, CETP, PLTP, LCAT. **Light green cluster**: angiotensinogen, Beta-2-glycoprotein 1, pigment epithelium-derived factor, protein AMBP, zinc-alpha-2-glycoprotein, Ig alpha-1- chain C region, hemoglobin subunit alpha, hemopexin, galectin-3-binding protein, Alpha-2-macroglobulin, platelet factor 4, thymosin beta-4. **Orange cluster**: PG(36:3), plasma HDL-C, antiapoptotic activity. **Light blue cluster**: antiinflammatory activity, antithrombotic activity. (B) Mosaic structure-function model of HDL linking functional metrics to protein (orange), glycoprotein (green) and lipid (yellow) components. Individual HDL components found to be associated with functional metrics using global network analysis are shown within a circle. Individual functional metrics and HDL components associated to them are shown within separate rectangles.

Discussion

In this study, we applied proteomic, lipidomic and glycomic approaches paralleled by functional evaluations for profiling structure-function relationships across HDL in patients carrying GOF PCSK9 genetic variants as compared to dyslipidemic patients carrying genetic variants in LDLR treated or not treated with a statin, and to normolipidemic controls. Overall, our data reveal a remarkable distinction between FH-PCSK9 patients and both FH-LDLR patients and normolipidemic controls, suggesting that the pathology of GOF PCSK9 genetic variants is associated with specific alterations in HDL metabolism.

PCSK9 is involved in the regulation of HDL metabolism, affecting clearance of apoE-containing HDL via LDL-R in mice [10]. In our study, a non-significant reduction in HDL-C was observed in FH-PCSK9 patients, consistent with earlier data [2, 25, 26]. Our results show that the role of PCSK9 in dyslipidemia may go beyond its immediate effects on LDL-R activity and LDL-C levels [2], potentially including altered activities of LCAT and PLTP, key players of lipoprotein metabolism.

In addition to these metabolic alterations, several functional alterations were found in FH-PCSK9 HDL in our study, which were predominantly common to all FH groups. Indeed, HDL particles from all FH groups, independent of the underlying genetic variant, were less effective in attenuating apoptosis in endothelial cells relative to normolipidemic HDL. Although there is no data available on the antiapoptotic activity of HDL in FH, several studies highlight that in this metabolic disease, reduced HDL-C levels can be accompanied by a variety of HDL modifications, including oxidative damage [23, 53–55]. Our data further revealed deficiency of antioxidative activity of FH HDL, which was most pronounced in the presence of GOF PCSK9 genetic variants. Consistent with these data, defective antioxidative activity of HDL subfractions paralleled by compositional alterations resulting in elevated rigidity of the HDL surface lipid monolayer was reported in FH [23]. Similar to other atheroprotective properties, HDL capacity to blunt inflammatory response can be deficient in patients subjected to elevated oxidative stress and dyslipidemia [56, 57]. Consistent with this observation, FH-PCSK9 and ntFH-LDLR HDLs were defective in their capacity to reduce accumulation in LDL of proinflammatory oxPL in our study.

By contrast, no deficiency in the capacity of FH HDL to reduce collagen-induced platelet aggregation was found by us. Prior studies reveal that HDL isolated from patients with hypertriglyceridemia displays impaired activity against platelet aggregation [58]. However, antithrombotic activity of HDL was never evaluated in FH. HDL can remove cholesterol from peripheral macrophages and transport it to the liver in a process of reverse cholesterol transport [59, 60]. Several clinical studies reported that cholesterol efflux capacity of HDL was more closely associated with atherosclerotic burden than HDL-C [61, 62]. Although data

obtained in a murine model demonstrate that PCSK9 deficiency decreases serum cholesterol efflux capacity from macrophages [63], no change in cholesterol efflux capacity of HDL was found by us in patients with FH, consistent with earlier reports [22, 25].

In addition to these functional alterations, several compositional abnormalities, including enrichment in CE and depletion of FC and PL, were observed in HDL from all FH groups, in agreement with earlier data [23]. Such alterations typically reflect enhanced LCAT activity, which was however found to be reduced in FH HDL using a fluorescent activity assay, which is known to largely reflect LCAT mass rather than activity [64]. Moreover, large-scale analysis of the omics data established further distinction between FH-PCSK9 patients and controls.

First, proteomic analysis detected altered content of several proteins in FH-PCSK9 HDL. Interestingly, alterations in the content of haptoglobin were common to all the three FH groups. While increased plasma levels of haptoglobin are consistently associated with inflammation [65, 66], HDL dysfunction can be related to the presence of glycosylated haptoglobin–haemoglobin complex [67]. In addition, increased serum concentration of haptoglobin was found in hypercholesterolemia [68]. Mechanisms behind alterations of haptoglobin metabolism in hypercholesterolemia might involve induction of inflammatory cytokine release, which stimulates hepatocytes to synthesize this acute-phase protein. Serotransferrin is an iron-binding protein [69] whose content was elevated in HDL from FH-PCSK9 and tFH-LDLR patients. Although there are no studies of the effects of hypercholesterolemia on serotransferrin metabolism, an antiiflammatory treatment increased HDL content of transferrin in patients with rheumatoid arthritis [70]. The increased serotransferrin content of HDL observed by us could therefore reflect antiinflammatory effects of LDL-lowering in these groups. Next, apo A-IV content was increased in HDL from FH-PCSK9 and ntFH-LDLR groups. ApoA-IV is a multifunctional protein, which contributes to antioxidative activity and cholesterol efflux capacity of HDL. Consistent with our data, HDL3 from coronary artery disease (CAD) patients were enriched in apoA-IV [71]. Finally, we identified elevated content of complement C3 in both ntFH-LDLR and tFH-LDLR HDL. Consistent with this result, enrichment of HDL with complement components was reported in CAD [71]. Earlier studies documented relevance of complement components in promoting immune responses during atherogenesis [72].

Second, the N-glycome analysis of HDL revealed that the content of a single sialylated N-glycan GP13 specifically distinguished HDLs from the FH-PCSK9 and normolipidemic groups. By contrast, the content of four common sialylated N-glycans distinguished HDL of statin-treated or non-treated FH-LDLR groups from normolipidemic HDL. Compared to normolipidemic controls, HDL from FH patients carried elevated content of sialylated N-glycans containing one or two sialic acid residues but lacking fucose residues. Sialylated

glycans are well recognized to participate in diverse cellular events and are highly abundant in HDL [73, 74]. Although there are no studies of the HDL N-glycome in FH, conflicting results were reported in other clinical settings involving CAD and metabolic syndrome [73, 75]. Interestingly, desialylation of HDL can significantly attenuate its capacity to efflux cellular cholesterol [76]. Mechanisms that drive compositional transformation of FH HDL toward an enrichment in sialylated glycans lacking fucose residues are unclear.

Third, our study revealed distinct lipidomic profile of HDL in the FH-PCSK9 group. Notably, lysophospholipids were enriched in HDL isolated from FH-PCSK9 patients. Increased concentrations of LPC species were reported in plasma of FH patients [77]. Several studies document implication of proinflammatory LPCs in the pathogenesis of atherosclerosis [78–80]. Although underlying mechanisms of LPC increase in hypercholesterolemia remain unknown, plasma Lp-PLA2 activity is elevated in FH [81], potentially accounting for the enrichment in HDL of LPC species. Furthermore, we observed an overall depletion of several PL classes, including PA, PS, PG, PE and PCs, in FH-PCSK9 HDL as compared to both FH-LDLR patients and to normolipidemic controls. Similarly, depletion of several PL classes was found in FH-LDLR HDL as compared to normolipidemic controls. PLs represent a major bioactive lipid component of HDL, which contribute to multiple HDL functions [82]. Thus, deficient HDL functions found in the present study can be attributed to the reduction of HDL content of bioactive PLs. Consistent with these findings, lipidomic analysis showed elevated PL content in HDL from patients receiving PCSK9 inhibitors, suggesting that PCSK9 inhibition may restore HDL functions associated with PL depletion [83]. In parallel, SM (36:2), Cer (d18:1/26:0) and several TG species were enriched in PCSK9 HDL relative to normolipidemic controls. Similarly, Cer (d18:1/26:0) and several TG species were enriched in HDL from the both FH-LDLR groups as compared to the controls. Consistent with our data, sphingomyelin content of HDL3 was elevated in FH [23], concomitant with increased surface rigidity and reduced antioxidative capacity of HDL3 [17, 84]. Furthermore, plasma ceramides were associated with accelerated development of CAD [85, 86]. Finally, marked triglyceride enrichment of HDL particles reduced their anti-inflammatory activity following Intralipid^{TM} administration in humans [87].

Using network analysis, we attempted to identify relationships between HDL function and composition in FH resulting from genetic variants in PCSK9 and LDLR. We found that metrics of HDL function were specifically associated with multiple compositional features of HDL. Thus, antioxidative function of HDL was linked to the abundances of 17 components, including eight lipid species, eight glycans and one protein. In contrast, cholesterol efflux capacity of HDL was associated with the abundances of two proteins and activities of lipid transfer proteins, while antiapoptotic activity was only associated with the abundance of a single lipid species. Intriguingly, antiinflammatory and antithrombotic functions were

unrelated to HDL composition in our study; moreover, most of the HDL functions were not interrelated. These results are in agreement with previous study of structure-function relationships across HDL in patients with Type 2 diabetes and CAD [19].

Lipids, proteins and glycans contribute to biological activities of HDL, acting via several mechanisms [74, 88, 89]. In our study, increased HDL content of haptoglobin, serotransferrin and A2G2S2 glycan (GP13), and decreased content of several PL species, mainly PAs, together with increased content of LPC 20:1 and Cer (18:1-26:0), were observed in FH HDLs. These observations suggest that reduced biological activities of HDL in FH may arise from combined alterations of protein, lipid and glycan moieties. Together, these data allow us to propose a novel mosaic structure-function model of HDL in which each biological function of the lipoprotein is linked to a specific, potentially distinct or in part overlapping, set of individual components (Figure 6, B). Our study thereby provides a first glimpse into these complex associations in FH, which requires further study.

Despite its originality, our study is not free of limitations. FH-LDLR patients recruited for this study as dyslipidemic controls were treated or not by statins in a “real-life” clinical setting. To directly assess effects of statins on the parameters of interest, a separate group of FH patients needs to be enrolled before and after statin treatment. In addition, the study groups were not fully matched according to sex, although no significant differences in the sex ratio between the groups was observed. Finally, fluorescent activity assays employed may frequently reflect enzyme mass rather than activity.

Conclusions

In the context of atherosclerosis, mechanisms of how HDL function, composition and structure can be affected by PCSK9 activity are yet not understood. The present study for the first time documents altered HDL particle profile and functionality in patients with GOF PCSK9 genetic variants. Based on these data, we propose a mosaic structure-function model for the assessment of HDL biology in the context of FH.

Declarations of interest: AK is a co-author of two patents on the measurement and enhancement of HDL function. EB received honoraria from MSD, Astra Zeneca, Danone, GENFIT, Amgen, Sanofi-Aventis, Aegerion/Amryt, Lilly, Mylan, Novartis, Pfizer, Servier and AKCEA.

Acknowledgments: The authors would like to gratefully acknowledge Drs. Catherine Calzada and Monique Dufilho, for providing guidance and valuable comments for platelet isolation. HUVEC cells were a kind gift from Professor Stephane Hatem.

Authors' contributions:

AK, WLG, MG, MD, GL designed research studies; MD, ML, IG, LM, MPB, LMD, LP, EF, CF performed experiments and produced data; MC, MV, AC, MK, BC, EB, PG, DBR, RB recruited study subjects; MD, MP, LM performed data analyses; MD, AK wrote the manuscript. All authors have approved the final version of the manuscript.

Fundings:

This study was primarily supported by a Pfizer ASPIRE Research Grant in Cardiovascular Research. Continuous support provided by the National Institute for Health and Medical Research (INSERM) and Sorbonne University (Paris, France) is gratefully acknowledged. We are grateful to the Croatian Science Foundation for providing support to the project "GLYCARD: Glycosylation in Cardiovascular Diseases" (UIP-2019-04-5692).

References

1. Lagace TA, Curtis DE, Garuti R, et al (2006) Secreted PCSK9 decreases the number of LDL receptors in hepatocytes and in livers of parabiotic mice. J Clin Invest 116:2995–3005. https://doi.org/10.1172/JCI29383
2. Herbert B, Patel D, Waddington SN, et al (2010) Increased Secretion of Lipoproteins in Transgenic Mice Genetic Control. 1333–1339. https://doi.org/10.1161/ATVBAHA.110.204040
3. Kingwell B a, Chapman MJ, Kontush A, Miller NE (2014) HDL-targeted therapies: progress, failures and future. Nat Rev Drug Discov 13:445–64. https://doi.org/10.1038/nrd4279
4. Horton JD, Cohen JC, Hobbs HH (2007) Molecular biology of PCSK9: its role in LDL metabolism. Trends Biochem. Sci. 32:71–77
5. Schulz R, Schlüter KD (2017) PCSK9 targets important for lipid metabolism. Clin Res Cardiol Suppl 12:2–11. https://doi.org/10.1007/s11789-017-0085-0
6. Abifadel M, Varret M, Rabès J-P, et al (2003) Mutations in PCSK9 cause autosomal dominant hypercholesterolemia. Nat Genet 34:154–156. https://doi.org/10.1038/ng1161
7. Cameron J, Holla ØL, Ranheim T, et al (2006) Effect of mutations in the PCSK9 gene on the cell surface LDL receptors. Hum Mol Genet 15:1551–1558. https://doi.org/10.1093/hmg/ddl077
8. Poirier S, Mayer G, Poupon V, et al (2009) Dissection of the endogenous cellular pathways of PCSK9-induced low density Lipoprotein receptor degradation. Evidence for an intracellular route. J Biol Chem 284:28856–28864. https://doi.org/10.1074/jbc.M109.037085
9. Shioji K, Mannami T, Kokubo Y, et al (2004) Genetic variants in PCSK9 affect the cholesterol level in Japanese. J Hum Genet 49:109–114. https://doi.org/10.1007/s10038-003-0114-3
10. Choi S, Korstanje R (2013) Proprotein convertases in high-density lipoprotein metabolism. Biomark Res 1:27. https://doi.org/10.1186/2050-7771-1-27
11. Jin W, Wang X, Millar JS, et al (2007) Hepatic Proprotein Convertases Modulate HDL Metabolism. Cell Metab 6:129–136. https://doi.org/10.1016/j.cmet.2007.07.009
12. Burnap SA, Sattler K, Pechlaner R, et al (2021) PCSK9 Activity Is Potentiated Through HDL Binding. Circ Res 129:1039–1053. https://doi.org/10.1161/CIRCRESAHA.121.319272
13. Burnap SA, Mayr M (2021) Lipoprotein compartmentalisation as a regulator of PCSK9 activity. J Mol Cell Cardiol 155:21–24. https://doi.org/10.1016/j.yjmcc.2021.02.004
14. Dafnis I, Tsouka AN, Gkolfinopoulou C, et al (2022) PCSK9 is minimally associated with HDL but impairs the anti-atherosclerotic HDL effects on endothelial cell activation. J Lipid Res 63:100272. https://doi.org/10.1016/j.jlr.2022.100272
15. Kontush A (2014) HDL-mediated mechanisms of protection in cardiovascular disease. Cardiovasc Res 103:341–9. https://doi.org/10.1093/cvr/cvu147
16. Voight BF, Peloso GM, Orho-Melander M, et al (2012) Plasma HDL cholesterol and risk of myocardial infarction: a mendelian randomisation study. Lancet (London, England) 380:572–80. https://doi.org/10.1016/S0140-6736(12)60312-2
17. Camont L, Lhomme M, Rached F, et al (2013) Small, dense high-density lipoprotein-3 particles are enriched in negatively charged phospholipids: relevance to cellular cholesterol efflux, antioxidative, antithrombotic, anti-inflammatory, and antiapoptotic functionalities. Arterioscler Thromb Vasc Biol 33:2715–23. https://doi.org/10.1161/ATVBAHA.113.301468
18. Kontush a., Tubeuf E, Le Goff W, et al (2015) Phosphatidylserine potently enhances anti-inflammatory activities of reconstituted HDL. Atherosclerosis 241:e30. https://doi.org/10.1016/j.atherosclerosis.2015.04.112
19. Cardner M, Yalcinkaya M, Goetze S, et al (2020) Structure-function relationships of HDL in diabetes and coronary heart disease. JCI Insight 5:1–18.

https://doi.org/10.1172/jci.insight.131491
20. Rached F, Santos RD, Camont L, et al (2014) Defective functionality of HDL particles in familial apoA-I deficiency: relevance of alterations in HDL lipidome and proteome. J Lipid Res 55:2509–2520. https://doi.org/10.1194/jlr.M051631
21. Rached F, Lhomme M, Camont L, et al (2015) Defective Functionality of Small, Dense HDL3 Subpopulations in ST Segment Elevation Myocardial Infarction: Relevance of Enrichment in Lysophosphatidylcholine, Phosphatidic Acid and Serum Amyloid A. Biochim Biophys Acta 1851:1254–1261. https://doi.org/10.1016/j.bbalip.2015.05.007
22. Bellanger N, Orsoni A, Julia Z, et al (2011) Atheroprotective reverse cholesterol transport pathway is defective in familial hypercholesterolemia. Arterioscler Thromb Vasc Biol 31:1675–1681. https://doi.org/10.1161/ATVBAHA.111.227181
23. Hussein H, Saheb S, Couturier M, et al (2016) Small, dense high-density lipoprotein 3 particles exhibit defective antioxidative and anti-inflammatory function in familial hypercholesterolemia: Partial correction by low-density lipoprotein apheresis. J Clin Lipidol 10:124–133. https://doi.org/10.1016/j.jacl.2015.10.006
24. Di Taranto MD, De Falco R, Guardamagna O, et al (2019) Lipid profile and genetic status in a familial hypercholesterolemia pediatric population: Exploring the LDL/HDL ratio. Clin Chem Lab Med 57:1102–1110. https://doi.org/10.1515/cclm-2018-1037
25. Abifadel M, Guerin M, Benjannet S, et al (2012) Identification and characterization of new gain-of-function mutations in the PCSK9 gene responsible for autosomal dominant hypercholesterolemia. Atherosclerosis 223:394–400. https://doi.org/10.1016/j.atherosclerosis.2012.04.006
26. Naoumova RP, Tosi I, Patel D, et al (2005) Severe Hypercholesterolemia in Four British Families With the D374Y Mutation in the PCSK9 Gene Long-Term Follow-Up and Treatment Response. 2654–2660. https://doi.org/10.1161/01.ATV.0000190668.94752.ab
27. Palumbo M, Giammanco A, Purrello F, et al (2022) Effects of PCSK9 inhibitors on HDL cholesterol efflux and serum cholesterol loading capacity in familial hypercholesterolemia subjects: a multi-lipid-center real-world evaluation. Front Mol Biosci 9:. https://doi.org/10.3389/fmolb.2022.925587
28. Ingueneau C, Hollstein T, Grenkowitz T, et al (2020) Treatment with PCSK9 inhibitors induces a more anti-atherogenic HDL lipid profile in patients at high cardiovascular risk. Vascul Pharmacol 135:106804. https://doi.org/10.1016/j.vph.2020.106804
29. Abifadel M, Guerin M, Benjannet S, et al (2012) Identification and characterization of new gain-of-function mutations in the PCSK9 gene responsible for autosomal dominant hypercholesterolemia. Atherosclerosis 223:394–400. https://doi.org/10.1016/j.atherosclerosis.2012.04.006
30. Marmontel O, Charrière S, Simonet T, et al (2018) Single, short in-del, and copy number variations detection in monogenic dyslipidemia using a next-generation sequencing strategy. Clin Genet 94:132–140. https://doi.org/10.1111/cge.13250
31. Marmontel O, Rollat-Farnier PA, Wozny A, et al (2020) Development of a new expanded next-generation sequencing panel for genetic diseases involved in dyslipidemia. Clin Genet 98:589–594. https://doi.org/10.1111/cge.13832
32. Reeskamp LF, Tromp TR, Defesche JC, et al (2021) Next-generation sequencing to confirm clinical familial hypercholesterolemia. Eur J Prev Cardiol 28:875–883. https://doi.org/10.1093/eurjpc/zwaa451
33. Huijgen R, Sjouke B, Vis K, et al (2012) Genetic variation in APOB, PCSK9, and ANGPTL3 in carriers of pathogenic autosomal dominant hypercholesterolemic mutations with unexpected low LDL-Cl Levels. Hum Mutat 33:448–55. https://doi.org/10.1002/humu.21660
34. Pussinen PJ, Jauhiainen M, Vilkuna-rautiainen T, et al (2004) Periodontitis decreases the antiatherogenic potency of high density lipoprotein. 45:. https://doi.org/10.1194/jlr.M300250-JLR200
35. Chapman MJ, Goldstein S, Lagrange D, Laplaud PM (1981) A density gradient ultracentrifugal procedure for the isolation of the major lipoprotein classes from human

serum. J Lipid Res 22:339–358
36. Guerin M, Le Goff W, Frisdal E, et al (2003) Action of ciprofibrate in type IIB hyperlipoproteinemia: Modulation of the atherogenic lipoprotein phenotype and stimulation of high-density lipoprotein-mediated cellular cholesterol efflux. J Clin Endocrinol Metab 88:3738–3746. https://doi.org/10.1210/jc.2003-030191
37. Robins SJ, Lyass A, Brocia RW, et al (2013) Plasma lipid transfer proteins and cardiovascular disease . The Framingham Heart Study. Atherosclerosis 228:230–236. https://doi.org/10.1016/j.atherosclerosis.2013.01.046
38. Calzada C, V??ricel E, Colas R, et al (2013) Inhibitory effects of in vivo oxidized high-density lipoproteins on platelet aggregation: Evidence from patients with abetalipoproteinemia. FASEB J 27:2855–2861. https://doi.org/10.1096/fj.12-225169
39. Zakiev E, Rached F, Lhomme M, et al (2019) Distinct phospholipid and sphingolipid species are linked to altered HDL function in apolipoprotein A-I deficiency. J Clin Lipidol 13:468-480.e8. https://doi.org/10.1016/j.jacl.2019.02.004
40. Kontush A, de Faria EC, Chantepie S, Chapman MJ (2005) A normotriglyceridemic, low HDL-cholesterol phenotype is characterised by elevated oxidative stress and HDL particles with attenuated antioxidative activity. Atherosclerosis 182:277–85. https://doi.org/10.1016/j.atherosclerosis.2005.03.001
41. Hansel B, Girerd X, Bonnefont-Rousselot D, et al (2011) Blood Pressure-Lowering Response to Amlodipine as a Determinant of the Antioxidative Activity of Small, Dense HDL3. Am J Cardiovasc Drugs 11:317–325. https://doi.org/10.2165/11592280-000000000-00000
42. Villard EF, Ei Khoury P, Frisdal E, et al (2013) Genetic determination of plasma cholesterol efflux capacity is gender-specific and independent of HDL-cholesterol levels. Arterioscler Thromb Vasc Biol 33:822–828. https://doi.org/10.1161/ATVBAHA.112.300979
43. Navab M, Hama SY, Hough GP, et al (2001) A cell-free assay for detecting HDL that is dysfunctional in preventing the formation of or inactivating oxidized phospholipids. J Lipid Res 42:1308–1317
44. Schilcher I, Stadler JT, Lechleitner M, et al (2021) Endothelial lipase modulates paraoxonase 1 content and arylesterase activity of HDL. Int J Mol Sci 22:1–15. https://doi.org/10.3390/ijms22020719
45. Gordon SM, Deng J, Lu LJ, Davidson WS (2010) Proteomic Characterization of Human Plasma High Density Lipoprotein Fractionated by Gel Filtration Chromatography research articles. 5239–5249
46. Ugrina I, Trbojević Akmačić I, Lauc G, et al (2015) High-throughput glycomics: Optimization of sample preparation. Biochem 80:934–942. https://doi.org/10.1134/s0006297915070123
47. Pučić-Baković M, Gudelj I, Lauc G, et al (2019) Glycosylation of human plasma lipoproteins reveals a high level of diversity, which directly impacts their functional properties. Biochim Biophys Acta - Mol Cell Biol Lipids 1864:643–653. https://doi.org/10.1016/j.bbalip.2019.01.005
48. Cooper CA, Gasteiger E, Packer NH (2001) GlycoMod - A software tool for determining glycosylation compositions from mass spectrometric data. Proteomics 1:340–349. https://doi.org/10.1002/1615-9861(200102)1:2<340::AID-PROT340>3.0.CO;2-B
49. Dell A, Ceroni A, Haslma SM, et al (2008) GlycoWorkbench: a tool for the computer-assisted annotation of mass spectra of glycans. J Proteome Res 7:1650–1659. https://doi.org/10.1021/pr7008252
50. Paul Shannon 1, Andrew Markiel 1, Owen Ozier, 2 Nitin S. Baliga, 1 Jonathan T. Wang, 2 Daniel Ramage 2, et al (1971) Cytoscape: A Software Environment for Integrated Models. Genome Res 13:426. https://doi.org/10.1101/gr.1239303.metabolite
51. Gao J, Tarcea VG, Karnovsky A, et al (2010) Metscape: A Cytoscape plug-in for visualizing and interpreting metabolomic data in the context of human metabolic

networks. Bioinformatics 26:971–973. https://doi.org/10.1093/bioinformatics/btq048
52. Benjamini Y, Hochberg Y (1995) Controlling the False Discovery Rate: A Practical and Powerful Approach to Multiple Testing. J R Stat Soc Ser B 57:289–300. https://doi.org/10.1111/j.2517-6161.1995.tb02031.x
53. Koizumi J, Inazu A, Fujita H, et al (1988) Removal of apolipoprotein E-enriched high density lipoprotein by LDL-apheresis in familial hypercholesterolaemia: a possible activation of the reverse cholesterol transport system. Atherosclerosis 74:1–8. https://doi.org/10.1016/0021-9150(88)90184-0
54. Suades R, Padró T, Alonso R, et al (2013) Circulating CD45+/CD3+ lymphocyte-derived microparticles map lipid-rich atherosclerotic plaques in familial hypercholesterolaemia patients. Thromb Haemost 111:111–121. https://doi.org/10.1160/TH13-07-0612
55. Hansel B, Giral P, Nobecourt E, et al (2004) Metabolic syndrome is associated with elevated oxidative stress and dysfunctional dense high-density lipoprotein particles displaying impaired antioxidative activity. J Clin Endocrinol Metab 89:4963–71. https://doi.org/10.1210/jc.2004-0305
56. Perségol L, Vergès B, Gambert P, Duvillard L (2007) Inability of HDL from abdominally obese subjects to counteract the inhibitory effect of oxidized LDL on vasorelaxation. J Lipid Res 48:1396–1401. https://doi.org/10.1194/jlr.M600309-JLR200
57. Carnuta MG, Stancu CS, Toma L, et al (2017) Dysfunctional high-density lipoproteins have distinct composition , diminished anti- inflammatory potential and discriminate acute coronary syndrome from stable coronary artery disease patients. Sci Rep 1–13. https://doi.org/10.1038/s41598-017-07821-5
58. Deng Z, Liu B, Zhou J, et al (2003) [Effects of plasma very low density lipoprotein, low density lipoprotein and high density lipoprotein on platelet aggregation in endogenous hypertriglyceridemia]. Sichuan Da Xue Xue Bao Yi Xue Ban 34:704–7
59. Cuchel M, Rader DJ (2006) Macrophage reverse cholesterol transport: Key to the regression of atherosclerosis? Circulation 113:2548–2555. https://doi.org/10.1161/CIRCULATIONAHA.104.475715
60. Rader DJ, Alexander ET, Weibel GL, et al (2009) The role of reverse cholesterol transport in animals and humans and relationship to atherosclerosis. J Lipid Res 50 Suppl:S189-94. https://doi.org/10.1194/jlr.R800088-JLR200
61. Khera A V, Cuchel M, de la Llera-Moya M, et al (2011) Cholesterol efflux capacity, high-density lipoprotein function, and atherosclerosis. N Engl J Med 364:127–35. https://doi.org/10.1056/NEJMoa1001689
62. Rohatgi A, Khera A, Berry JD, et al (2014) HDL cholesterol efflux capacity and incident cardiovascular events. N Engl J Med 371:2383–93. https://doi.org/10.1056/NEJMoa1409065
63. Choi S, Aljakna A, Srivastava U, et al (2013) Decreased APOE-containing HDL subfractions and cholesterol efflux capacity of serum in mice lacking Pcsk9. Lipids Health Dis 12:112. https://doi.org/10.1186/1476-511X-12-112
64. Homan R, Esmaeil N, Mendelsohn L, Kato GJ (2013) A fluorescence method to detect and quantitate sterol esterification by lecithin:cholesterol acyltransferase. Anal Biochem 441:80–6. https://doi.org/10.1016/j.ab.2013.06.018
65. Chiellini C, Santini F, Marsili A, et al (2004) Serum haptoglobin: A novel marker of adiposity in humans. J Clin Endocrinol Metab 89:2678–2683. https://doi.org/10.1210/jc.2003-031965
66. De Pergola G, Di Roma P, Paoli G, et al (2007) Haptoglobin serum levels are independently associated with insulinemia in overweight and obese women. J Endocrinol Invest 30:399–403. https://doi.org/10.1007/BF03346317
67. Asleh R, Miller-Lotan R, Aviram M, et al (2006) Haptoglobin genotype is a regulator of reverse cholesterol transport in diabetes in vitro and in vivo. Circ Res 99:1419–1425. https://doi.org/10.1161/01.RES.0000251741.65179.56
68. Jugnam-Ang W, Pannengpetch S, Isarankura-Na-Ayudhya P, et al (2015) Retinol-binding protein 4 and its potential roles in hypercholesterolemia revealed by

proteomics. EXCLI J 14:999–1013. https://doi.org/10.17179/excli2015-478
69. Vickers KC, Remaley AT (2014) HDL and cholesterol: Life after the divorce? 1. J Lipid Res 55:4–12. https://doi.org/10.1194/jlr.R035964
70. Charles-Schoeman C, Gugiu GB, Ge H, et al (2018) Remodeling of the HDL proteome with treatment response to abatacept or adalimumab in the AMPLE trial of patients with rheumatoid arthritis. Atherosclerosis 275:107–114. https://doi.org/10.1016/j.atherosclerosis.2018.04.003
71. Vaisar T, Pennathur S, Green PS, et al (2007) Shotgun proteomics implicates protease inhibition and complement activation in the antiinflammatory properties of HDL. J Clin Invest 117:746–56. https://doi.org/10.1172/JCI26206
72. Oksjoki R, Kovanen PT, Pentikäinen MO (2003) Role of complement activation in atherosclerosis. Curr Opin Lipidol 14:477–482. https://doi.org/10.1097/00041433-200310000-00008
73. Zivkovic AM, Lee H, Guerrero A, et al (2015) Combined High-Density Lipoprotein Proteomic and Glycomic Profiles in Patients at Risk for Coronary Artery Disease. J Proteome Res 14:5109–5118. https://doi.org/10.1021/acs.jproteome.5b00730
74. Pirillo A, Svekla M, Catapano AL, et al (2020) Impact of Protein Glycosylation on Lipoprotein Metabolism and Atherosclerosis. Cardiovasc Res. https://doi.org/10.1093/cvr/cvaa252
75. Savinova O V., Fillaus K, Jing L, et al (2014) Reduced apolipoprotein glycosylation in patients with the metabolic syndrome. PLoS One 9:. https://doi.org/10.1371/journal.pone.0104833
76. Sukhorukov V, Gudelj I, Pučić-Baković M, et al (2019) Glycosylation of human plasma lipoproteins reveals a high level of diversity, which directly impacts their functional properties. Biochim Biophys Acta - Mol Cell Biol Lipids 1864:643–653. https://doi.org/10.1016/j.bbalip.2019.01.005
77. Stübiger G, Aldover-Macasaet E, Bicker W, et al (2012) Targeted profiling of atherogenic phospholipids in human plasma and lipoproteins of hyperlipidemic patients using MALDI-QIT-TOF-MS/MS. Atherosclerosis 224:177–186. https://doi.org/10.1016/j.atherosclerosis.2012.06.010
78. Law SH, Chan ML, Marathe GK, et al (2019) An updated review of lysophosphatidylcholine metabolism in human diseases. Int J Mol Sci 20:1–24. https://doi.org/10.3390/ijms20051149
79. Murugesan G, Rani MRS, Gerber CE, et al (2003) Lysophosphatidylcholine regulates human microvascular endothelial cell expression of chemokines. J Mol Cell Cardiol 35:1375–1384. https://doi.org/10.1016/j.yjmcc.2003.08.004
80. Li X, Wang L, Fang P, et al (2018) Lysophospholipids induce innate immune transdifferentiation of endothelial cells, resulting in prolonged endothelial activation. J Biol Chem 293:11033–11045. https://doi.org/10.1074/jbc.RA118.002752
81. Mattina A, Rosenbaum D, Bittar R, et al (2018) Lipoprotein-associated phospholipase A_2 activity is increased in patients with definite familial hypercholesterolemia compared with other forms of hypercholesterolemia. Nutr Metab Cardiovasc Dis 28:517–523. https://doi.org/10.1016/j.numecd.2018.01.012
82. Darabi M, Guillas-Baudouin I, Le Goff W, et al (2015) Therapeutic applications of reconstituted HDL: When structure meets function. Pharmacol Ther 157:28–42. https://doi.org/10.1016/j.pharmthera.2015.10.010
83. Hilvo M, Simolin H, Metso J, et al (2018) PCSK9 inhibition alters the lipidome of plasma and lipoprotein fractions. Atherosclerosis 269:159–165. https://doi.org/10.1016/j.atherosclerosis.2018.01.004
84. Kontush A, Therond P, Zerrad A, et al (2007) Preferential sphingosine-1-phosphate enrichment and sphingomyelin depletion are key features of small dense HDL3 particles: relevance to antiapoptotic and antioxidative activities. Arterioscler Thromb Vasc Biol 27:1843–9. https://doi.org/10.1161/ATVBAHA.107.145672
85. Iqbal J, Walsh MT, Hammad SM, Hussain MM (2017) Sphingolipids and Lipoproteins in Health and Metabolic Disorders. Trends Endocrinol Metab 28:506–518.

https://doi.org/10.1016/j.tem.2017.03.005
86. Kasumov T, Li L, Li M, et al (2015) Ceramide as a mediator of non-alcoholic fatty liver disease and associated atherosclerosis. PLoS One 10:1–26. https://doi.org/10.1371/journal.pone.0126910
87. Patel S, Puranik R, Nakhla S, et al (2009) Acute hypertriglyceridaemia in humans increases the triglyceride content and decreases the anti-inflammatory capacity of high density lipoproteins. Atherosclerosis 204:424–428. https://doi.org/10.1016/j.atherosclerosis.2008.07.047
88. Nofer J, Levkau B, Wolinska I, et al (2001) Suppression of Endothelial Cell Apoptosis by High Density Lipoproteins (HDL) and HDL-associated Lysosphingolipids *. 276:34480–34485. https://doi.org/10.1074/jbc.M103782200
89. de Souza J a, Vindis C, Nègre-Salvayre A, et al (2010) Small, dense HDL 3 particles attenuate apoptosis in endothelial cells: Pivotal role of apolipoprotein A-I. J Cell Mol Med 14:608–620. https://doi.org/10.1111/j.1582-4934.2009.00713.x